

## PHASE-LAG EFFECTS IN SKIN TISSUE DURING TRANSIENT HEATING

R. KUMAR<sup>\*</sup>, A.K. VASHISHTH and S. GHANGAS

Department of Mathematics, Kurukshetra University

Kurukshetra - 136119 Haryana, INDIA

E-mails: rajneesh\_kuk@rediffmail.com; akvashishth@kuk.ac.in; sunitikuk@gmail.com

A three-phase-lag (TPL) model is proposed to describe heat transfer in a finite domain skin tissue with temperature dependent metabolic heat generation. The Laplace transform method is applied to solve the problem. Three special types of heat flux are applied to the boundary of skin tissue for thermal therapeutic applications. The depth of tissue is influenced by the different oscillation heat flux. The comparison between the TPL and dual-phase-lag (DPL) models is analyzed and the effects of phase lag parameters ( $\tau_q$ ,  $\tau_t$  and  $\tau_v$ ) and material constant ( $k^*$ ) on the tissue temperature distribution are presented graphically.

**Key words:** bioheat transfer, skin tissue, three-phase-lag, Laplace transform, transient heating.

### 1. Introduction

The study of skin biothermomechanics is highly interdisciplinary involving bioheat transfer, biomechanics. The skin is characterized by its structure and properties. When thermal loading, such as contact heating, electromagnetic energy, acoustic energy, mechanical loading (force and deformation) is applied to skin tissue, then there are different skin states, including temperature, thermal damage/inflammation and stress/strain distribution.

Heat transfer is the primary mechanism affecting temperature. The transport of thermal energy in a living tissue is a complex process involving multiple phenomenological mechanisms. Skin bioheat transfer has been studied for many years in thermal therapies. The success of thermal therapies depends on the precise prediction and control of temperature, damage and stress distribution. A mathematical model can be used for optimizing thermal treatments by maximizing therapeutic effect while minimizing unwanted side effects.

Pennes' equation [1] is used widely to model such problems due to its simplicity which is based on classical Fourier's law and assumes that the speed of thermal energy transfer is infinite, in fact heat propagates with finite speed. Cattane and Vernotte [2-3] and DPL [4-5] model are increasingly applied to remove the paradox of infinite speed.

Roychoudhuri [6] established a generalized mathematical model that includes three-phase lags in the heat flux vector, the temperature gradient and in the thermal displacement gradient. The TPL model is very useful in the problems of nuclear boiling, phonon-electron interactions, phonon-scattering, etc., where the delay time  $\tau_q$  captures the thermal wave behavior, the delay time  $\tau_t$  captures the effect of phonon-electron interactions, the other delay time  $\tau_v$  is effective, since, the thermal displacement gradient is considered as a constitutive variable. Several studies have been made on the TPL model in thermoelasticity. For instance, Sur *et al.* [7] studied the TPL elasto-thermodiffusive response in an elastic solid under hydrostatic pressure. Kumar *et al.* [8] studied plane wave propagation in fractional thermoelastic materials with TPL heat transfer.

---

\* To whom correspondence should be addressed

In recent years [9-16], several studies have been devoted to the application of the DPL bioheat model to bioheat process modeling. Ahmadikia *et al.* [17-18] solved the parabolic and hyperbolic bioheat transfer models for constant, periodic and pulse train heat flux boundary conditions. Afrin *et al.* [19] used a generalized DPL model to investigate thermal damage induced by laser irradiation based on the non-equilibrium heat transfer.

Kengne *et al.* [20] applied a nonlinear one-dimensional temperature dependent blood-perfusion Pennes bioheat equation to predict temperature distribution in a finite biological tissue simultaneously subjected to oscillatory surface and spatial heating. Fazlali and Ahmadikia [21] obtained an analytical solution of the thermal wave model for skin tissue under arbitrary periodic boundary conditions. Shahnazari *et al.* [22] used Wrm-homotopy perturbation combination analysis to evaluate the heat transfer in tissue as a semi-infinite body and blood vessels as heat source have been considered.

Gupta *et al.* [23] obtained the solution of the modified nonlinear BHTE (bioheat transfer equation) by using finite the difference method. Askarizadeh and Ahmadikia [24] introduced the exact solution of the DPL BHTE in treating the transient heat transfer problems in skin tissue considering prevalent heating conditions in thermal therapy.

Kengne *et al.* [25] obtained an exact analytical solution of the BHTE with temperature-dependent blood perfusion, that describes the non uniform temperature distribution in biological tissue. Kumar *et al.* [26] studied the DPL model of bioheat transfer by using the Gaussian distribution source term under most generalized boundary condition during hyperthermia treatment and derived an approximate analytical solution by the finite element Legendre wavelet Galerkin method.

Work of Majchrzak *et al.* [27] is concerned with the numerical modeling of skin tissue heating to describe the analyzed process of the system of three generalized DPL equations corresponding to the successive layers of the skin. Jasinski *et al.* [28] presented a numerical analysis of thermal processes proceeding in a soft tissue subjected to a laser irradiation.

Kumar and Rai [29] studied the DPL model for multilayer tissues under the most generalized boundary condition with a modified Gaussian distribution heat source. Agrawal and Pardasani [30] proposed a finite element model to study temperature distribution in skin and deep tissue of elliptical tapered shape human limb.

The purpose of the present work is to study a finite length skin tissue during transient heating with temperature dependent metabolic heat generation. The TPL model of heat conduction is utilized to model the bioheat transfer equation. Thermal wave (TW) and DPL models can be obtained as particular cases of the TPL model by taking  $\tau_q = 0, k^* = 0$  and  $k^* = 0$ , respectively. The problem is solved analytically and solution of DPL, TW, Pennes' BHTE can be obtained by replacing an appropriate set of coefficients in the solution of TPL BHTE. The effects of relaxation times ( $\tau_q, \tau_t$  and  $\tau_v$ ) and material constant ( $k^*$ ) are observed on the tissue temperature distribution, the blood perfusion rate and the depth of tissue is influenced by the oscillation heat flux. The results obtained from the TPL model for limiting cases are compared with the results of the DPL model [24] and these are in good agreement, but with dimensionless blood perfusion rates, the temperature profile at skin surface shows different behavior in both models.

## 2. Formulation of the problem

A finite domain with a thickness of  $L$  cm of skin tissue is taken whose bottom boundary is assumed to be thermally insulated and the surface is subjected to constant and transient heat flux at time  $t > 0$ . For BHTE corresponding to the TPL model, the metabolic heat generation is temperature dependent and blood perfusion rate is considered constant. In the case of Pennes, TW, and DPL models blood perfusion rate and metabolic heat generation are considered constant, without any external heat sources.

**Initial conditions**

$$T(x, 0) = T_0, \quad \frac{\partial T}{\partial t}(x, 0) = 0, \quad \frac{\partial^2 T}{\partial t^2}(x, 0) = 0. \quad (2.1)$$

**Boundary conditions**

$$-kT_x(0, t) = q_0, \quad q_0[U(t) - U(t - \tau_i)], \quad q_0 e^{i\omega t}, \quad (2.2)$$

$$T_x(L, t) = 0. \quad (2.3)$$

**Pennes model**

Pennes' [1] bioheat transfer equation in living biological tissues is

$$\rho c \frac{\partial T}{\partial t} = -\frac{\partial q}{\partial x} + \omega_b \rho_b c_b (T_a - T) + q_m. \quad (2.4)$$

The conduction term in Eq.(2.4) is based on classical Fourier's law

$$q = -k \frac{\partial T}{\partial x}. \quad (2.5)$$

Using Eq.(2.5) in Eq.(2.4), Pennes' equation can be expressed as

$$\frac{\partial T}{\partial t} + \frac{\omega_b \rho_b c_b}{\rho c} (T - T_a) = \alpha \frac{\partial^2 T}{\partial x^2} + \frac{q_m}{\rho c}. \quad (2.6)$$

**Thermal wave model**

Thermal wave model of the BHTE has been proposed based on single-phase-lag and a linear extension of Fourier's law

$$q + \tau_q \frac{\partial q}{\partial t} = -k \frac{\partial T}{\partial x} \quad (2.7)$$

where relaxation time  $\tau_q$  represents the time needed to establish the heat flux when a temperature gradient is suddenly imposed.

Using Eq.(2.7) in Eq.(2.4), the TW model BHTE is obtained as

$$\tau_q \frac{\partial^2 T}{\partial t^2} + \left( 1 + \frac{\omega_b \rho_b c_b}{\rho c} \tau_q \right) \frac{\partial T}{\partial t} + \frac{\omega_b \rho_b c_b}{\rho c} (T - T_a) = \alpha \frac{\partial^2 T}{\partial x^2} + \frac{q_m}{\rho c}. \quad (2.8)$$

**Dual-phase-lag model**

Tzou [4] proposed a two phase lag model in order to capture the effect of micro-structural interactions along with the fast transient effects in the following form

$$q(x, t + \tau_q) = -k \nabla T(x, t + \tau_t). \quad (2.9)$$

This relation leads to the following DPL model of the bioheat equation

$$\tau_q \frac{\partial^2 T}{\partial t^2} + \left( I + \frac{\omega_b \rho_b c_b}{\rho c} \tau_q \right) \frac{\partial T}{\partial t} + \frac{\omega_b \rho_b c_b}{\rho c} (T - T_a) = \alpha \left( I + \tau_t \frac{\partial}{\partial t} \right) \frac{\partial^2 T}{\partial x^2} + \frac{q_m}{\rho c}. \quad (2.10)$$

### Three-phase-lag model

Green and Naghdi [31-32], developed a model which includes the temperature gradient and thermal displacement gradient and proposed a heat conduction law as

$$q = -[k \nabla T + k^* \nabla v], \quad (2.11)$$

where  $\nabla v$  ( $\dot{v} = T$ ) is the thermal displacement gradient.

Introducing the phase-lags to the heat flux vector ( $q$ ), the temperature gradient ( $\nabla T$ ) and the thermal displacement gradient ( $\nabla v$ ), the following generalized constitutive equation is proposed to describe the lagging behavior for heat conduction Roy Choudhuri [6]

$$q(x, t + \tau_q) = -[k \nabla T(x, t + \tau_t) + k^* \nabla v(x, t + \tau_v)]. \quad (2.12)$$

Taylor's series expansion of Eq.(2.12) leads to the following generalized heat conduction law

$$q + \tau_q \frac{\partial q}{\partial t} = -\left[ k \left( \nabla T + \tau_t \frac{\partial}{\partial t} (\nabla T) \right) + k^* \left( \nabla v + \tau_v \frac{\partial}{\partial t} (\nabla v) \right) \right], \quad (2.13)$$

$$i.e. \left( I + \tau_q \frac{\partial}{\partial t} \right) q = -\left[ \tau_v^* \nabla T + k \tau_t \frac{\partial}{\partial t} (\nabla T) + k^* \nabla v \right] \quad (2.14)$$

where  $\tau_v^* = k + k^* \tau_v$ .

Time derivative of Eq.(2.14) leads to

$$\left( I + \tau_q \frac{\partial}{\partial t} \right) \dot{q} = -\left[ \tau_v^* \frac{\partial}{\partial t} + k \tau_t \frac{\partial^2}{\partial t^2} + k^* \right] \nabla T. \quad (2.15)$$

Using Eq.(2.15) in Eq.(2.4), the following BHTE is obtained corresponding to the TPL model

$$\left( I + \tau_q \frac{\partial}{\partial t} \right) \left( \rho c \ddot{T} - \omega_b \rho_b c_b \frac{\partial}{\partial t} (T_a - T) - \dot{q}_m \right) = \left( \tau_v^* \frac{\partial}{\partial t} + k \tau_t \frac{\partial^2}{\partial t^2} + k^* \right) \frac{\partial^2 T}{\partial x^2}. \quad (2.16)$$

## 3. Solution of the problem

### 3.1. Constant heat flux

Introducing the dimensionless variable

$$\xi = \sqrt{\frac{\omega_0}{\alpha}} x, \quad x_L = \sqrt{\frac{\omega_0}{\alpha}} L, \quad \theta(\xi, \eta) = \frac{T(x, t) - T_a}{q_0} \sqrt{\frac{\omega_0}{\alpha}} k, \quad \eta = \omega_0 t, \quad (3.1)$$

$$\tau_{q'} = \omega_0 \tau_q, \quad \tau_{t'} = \omega_0 \tau_t, \quad \tau_{v'} = \omega_0 \tau_v, \quad \Gamma_i = \omega_0 \tau_i, \quad p_m = \frac{Q_0 \alpha}{T_0 \omega_0 k}, \quad \psi = \sqrt{\frac{\alpha}{\omega_0}} \frac{q_m}{q_0},$$

where  $\omega_0 = \frac{\omega_b \rho_b c_b}{\rho c}$ .

For all practical purposes Mitchel *et al.* [33], the dependence of metabolic heat generation can be approximated as a linear function of local tissue temperature as follows

$$q_m = Q_0 (1 + (T - T_0)/10),$$

where

$$Q_0 = Q_{m0} [1 + 0.1(T_w - 37)].$$

A dimensionless form of the BHTE corresponding to the TPL, DPL, TW, and Pennes' model is

$$A \frac{\partial^3 \theta}{\partial \eta^3} + B \frac{\partial^2 \theta}{\partial \eta^2} + C \frac{\partial \theta}{\partial \eta} + D\theta = \left( E \frac{\partial^2}{\partial \eta^2} + F \frac{\partial}{\partial \eta} + G \right) \frac{\partial^2 \theta}{\partial \xi^2} + \hat{\psi}, \quad (3.2)$$

with initial conditions

$$\theta(\xi, 0) = 0, \quad \theta_\eta(\xi, 0) = 0, \quad \theta_{\eta\eta}(\xi, 0) = 0, \quad (3.3)$$

and boundary conditions

$$\theta_\xi(0, \eta) = -1, \quad \theta_\xi(x_L, \eta) = 0, \quad (3.4)$$

where  $\hat{\psi}$  is zero in the case of the TPL model and  $\psi$  for other models.

By taking the Laplace transform of Eq.(3.2) and applying the initial conditions (3.3), the following ordinary differential equation is obtained

$$\frac{d^2 \bar{\theta}}{d\xi^2} - \delta \bar{\theta} = 0, \quad (3.5)$$

where

$$\delta = \frac{s(1 + As)(s + C)}{Es^2 + Fs + G}.$$

The exact solution of Eq.(3.5), by using the Laplace transform of boundary conditions (3.4), is

$$\bar{\theta}(\xi, s) = \frac{\cosh[\sqrt{\delta}(\xi - x_L)]}{s\sqrt{\delta} \sinh(\sqrt{\delta}x_L)}. \quad (3.6)$$

The inverse Laplace transforms of  $\bar{\theta}(\xi, s)$  can be obtained from the following Bromwich contour integration [34] Eq.(3.7)

$$\theta(\xi, \eta) = \frac{1}{2\pi i} \lim_{l \rightarrow \infty} \int_{\gamma - il}^{\gamma + il} e^{\eta s} \bar{\theta}(\xi, s) ds. \quad (3.7)$$

Using the inversion theorem, the inverse Laplace transform of Eq.(3.6) is

$$\theta(\xi, \eta) = \frac{I}{2\pi i} \int_{\gamma-i\infty}^{\gamma+i\infty} \left[ \frac{\cosh[\sqrt{\delta}(\xi - x_L)]}{s\sqrt{\delta} \sinh(\sqrt{\delta}x_L)} \right] e^{\eta s} ds. \tag{3.8}$$

By using Bromwich contour integration [34], temperature distribution (TPL model) in skin tissue is

$$\begin{aligned} \theta(\xi, \eta) = & \left( \frac{\eta G}{x_L C} + \frac{I}{2x_L} - \frac{\xi}{2} - \frac{\xi^2}{2x_L} \right) + \frac{(EC^2 - CF + G)}{C^2 x_L (I - AC)} e^{-C\eta} + \frac{(E - AF + A^2 G)}{x_L (AC - I)} e^{-\frac{\eta}{A}} \\ & + \sum_{m=1}^3 \sum_{n=1}^{\infty} \frac{2 \cos\left( (\xi - x_L) \frac{\lambda_n}{x_L} \right) (Es_{nm}^2 + Fs_{nm} + G)}{x_L \cos(\lambda_n) \left[ s_{nm} (3As_{nm}^2 + (2AC + 2Eb_n + 2)s_{nm} + C + Fb_n) \right]} e^{s_{nm}\eta}. \end{aligned} \tag{3.9}$$

Temperature distribution for the Pennes, TW and DPL model is

$$\begin{aligned} \theta(\xi, \eta) = & \frac{\cosh(\xi - x_L)}{\sinh x_L} + \psi \left( I + \frac{e^{-\eta} - Be^{-\frac{\eta}{B}}}{B - I} \right) + \frac{(I - E)e^{-\eta} + (E - B)e^{-\frac{\eta}{B}}}{x_L (B - I)}, \\ & \sum_{m=1}^2 \sum_{n=1}^{\infty} \frac{2 \cos\left[ (\xi - x_L) \lambda_n / x_L \right]}{x_L \cos \lambda_n} \times \left[ \frac{(I + Es_{nm}) e^{s_{nm}\eta}}{s_{nm} (2Bs_{nm} + B + I + Eb_n)} \right], \end{aligned} \tag{3.10}$$

where

$$b_n = \left( \frac{\lambda_n}{x_L} \right)^2, \quad \lambda_n = n\pi, \quad n = 1, 2, \dots$$

The roots of Eq.(3.11)

$$as_{nm}^3 + bs_{nm}^2 + cs_{nm} + d = 0, \tag{3.11}$$

are calculated by using MATLAB 8.1 software.

Table 1. Coefficients of (a) Eq.(3.2), (b) Eq.(3.18), (c) Eq.(3.11), (d) Eq.(3.24).

Bioheat models	Coefficients						
	A	B	C	D	E	F	G
(a)							
TPL	$\tau_{q'}$	$I + l_m \tau_{q'}$	$l_m$	$0$	$\tau_{t'}$	$I + \frac{k^* \tau_{v'}}{k\omega_0}$	$\frac{k^*}{k\omega_0}$
DPL	$0$	$\tau_{q'}$	$I + \tau_{q'}$	$I$	$0$	$\tau_{t'}$	$I$
TW	$0$	$\tau_{q'}$	$I + \tau_{q'}$	$I$	$0$	$0$	$I$
Pennes	$0$	$0$	$I$	$I$	$0$	$0$	$I$

Bioheat models	Coefficients						
(b)	A'	B'	C'	D'	E'	F'	G'
TPL	$\tau_l$	$1 + m_m \tau_l$	$m_m$	$0$	$\tau_2$	$1 + \frac{k^* \tau_3}{k\omega}$	$\frac{k^*}{k\omega}$
DPL	$0$	$\tau_l$	$1 + \lambda_0 \tau_l$	$\lambda_0$	$0$	$\tau_2$	$1$
TW	$0$	$\tau_l$	$1 + \lambda_0 \tau_l$	$\lambda_0$	$0$	$0$	$1$
Pennes	$0$	$0$	$1$	$\lambda_0$	$0$	$0$	$1$

Bioheat models	Coefficients			
(c)	a	b	c	d
TPL	A	$1 + AC + b_n E$	$C + b_n F$	$b_n G$
DPL/TW/Pennes	0	B	$1 + B + E b_n$	$1 + b_n$

Bioheat models	Coefficients			
(d)	a'	b'	c'	d'
TPL	A'	$1 + A'C' + b_n E'$	$C' + b_n F'$	$b_n G'$
DPL/TW/Pennes	0	B'	$1 + B' + E' b_n$	$D' + b_n$

where  $l_m = 1 - 0.1T_0 \rho_m$  and  $m_m = \lambda_0 - 0.1T_0 \rho_m$ .

### 3.2. Pulse train heat flux

A dimensionless form of boundary conditions (2.2) and (2.3) is

$$-\frac{\partial \theta}{\partial \xi}(0, \eta) = U \left( \frac{\eta}{\omega_0} \right) - U \left( \frac{1}{\omega_0} (\eta - \Gamma_i) \right), \quad \frac{\partial \theta}{\partial \xi}(x_L, \eta) = 0. \quad (3.12)$$

In the Laplace domain, the transformed forms of boundary conditions are

$$-\frac{d\bar{\theta}(0, s)}{d\xi} = \frac{1 - e^{-\Gamma_i s}}{s}, \quad \frac{d\bar{\theta}(x_L, s)}{d\xi} = 0. \quad (3.13)$$

In this case, an analytical solution is obtained by applying the pulse train boundary condition to the previous solution. Temperature distribution for this case is

$$\bar{\theta}(\xi, s) = \frac{1 - e^{-\Gamma_i s}}{s} \frac{\cosh[\sqrt{\delta}(\xi - x_L)]}{\sqrt{\delta} \sinh(\sqrt{\delta} x_L)}. \quad (3.14)$$

The following property of the inverse Laplace transform is employed to find the inverse Laplace transform of Eq.(3.14)

$$e^{-\Gamma_i s} \bar{\theta}(\xi, s) = \begin{cases} 0, & \text{for } \eta < \Gamma_i \\ \theta(\xi, \eta - \Gamma_i), & \text{for } \eta \geq \Gamma_i. \end{cases}$$

Therefore, the inverse Laplace transform of Eq.(3.14) is obtained for  $\eta < \Gamma_i$

$$\theta(\xi, \eta) = \left( \frac{\eta G}{x_L C} + \frac{I}{2x_L} - \frac{\xi}{2} - \frac{\xi^2}{2x_L} \right) + \frac{(EC^2 - CF + G)}{C^2 x_L (I - AC)} e^{-C\eta} + \frac{(E - AF + A^2 G)}{x_L (AC - I)} e^{-\frac{\eta}{A}} + \sum_{m=1}^3 \sum_{n=1}^{\infty} \frac{2 \cos\left(\left(\xi - x_L\right) \frac{\lambda_n}{x_L}\right) (Es_{nm}^2 + Fs_{nm} + G)}{x_L \cos(\lambda_n) \left[ s_{nm} (3As_{nm}^2 + (2AC + 2Eb_n + 2)s_{nm} + C + Fb_n) \right]} e^{s_{nm}\eta}, \quad (3.15)$$

and for  $\eta \geq \Gamma_i$ ,

$$\theta(\xi, \eta) = \frac{\Gamma_i G}{x_L C} + \frac{EC^2 - CF + G}{C^2 x_L (I - AC)} \left( I - e^{C\Gamma_i} \right) e^{-C\eta} + \frac{E - AF + A^2 G}{x_L (AC - I)} \left( I - e^{\frac{\Gamma_i}{A}} \right) e^{-\frac{\eta}{A}} + \sum_{m=1}^3 \sum_{n=1}^{\infty} \frac{2 \cos\left(\left(\xi - x_L\right) \frac{\lambda_n}{x_L}\right) (Es_{nm}^2 + Fs_{nm} + G)}{x_L \cos(\lambda_n) \left[ s_{nm} (3As_{nm}^2 + (2AC + 2Eb_n + 2)s_{nm} + C + Fb_n) \right]} \left( I - e^{-s_{nm}\Gamma_i} \right) e^{s_{nm}\eta} \quad (3.16)$$

where

$$b_n = \left( \frac{\lambda_n}{x_L} \right)^2, \quad \lambda_n = n\pi, \quad n = 1, 2, \dots$$

### 3.3. Periodic heat flux

Dimensionless quantities are as follows

$$\xi = \sqrt{\frac{\omega}{\alpha}} x, \quad \eta = \omega t, \quad \theta(\xi, \eta) = k \frac{T(x, t) - T_a}{q_0} \sqrt{\frac{\omega}{\alpha}}, \quad \lambda_0 = \frac{\omega_0}{\omega}, \quad (3.17)$$

$$x_L = \sqrt{\frac{\omega}{\alpha}} L, \quad \tau_1 = \omega \tau_q, \quad \tau_2 = \omega \tau_t, \quad \tau_3 = \omega \tau_v, \quad p_m = \frac{Q_0}{\rho c \omega T_0}, \quad \phi = \sqrt{\frac{k}{\rho c \omega}} \frac{q_m}{q_0}.$$

The dimensionless forms of the bioheat transfer equation corresponding to the TPL, DPL, TW and Pennes' models and boundary conditions respectively are

$$A' \frac{\partial^3 \theta}{\partial \eta^3} + B' \frac{\partial^2 \theta}{\partial \eta^2} + C' \frac{\partial \theta}{\partial \eta} + D' \theta = \left( E' \frac{\partial^2}{\partial \eta^2} + F' \frac{\partial}{\partial \eta} + G' \right) \frac{\partial^2 \theta}{\partial \xi^2} + \hat{\phi}, \quad (3.18)$$

$$\theta_{\xi}(0, \eta) = -e^{i\eta}, \quad \theta_{\xi}(\xi, \eta) = 0, \quad (3.19)$$

where  $\hat{\phi}$  is 0 for the TPL model and  $\phi$  for other models.

Applying the Laplace transform to Eq.(3.18), the following ordinary differential equation is obtained

$$\frac{d^2 \bar{\theta}}{d\xi^2} - \delta' \bar{\theta} = 0, \quad (3.20)$$

where

$$\delta' = \frac{s(s + C')(I + A's)}{E's^2 + F's + G'}.$$

The solution of Eq.(3.20), by using the Laplace transform of Eq.(3.19), is

$$\bar{\theta}(\xi, s) = \frac{\cosh\left[\sqrt{\delta'}(\xi - x_L)\right]}{(s-i)\sqrt{\delta'} \sinh\left(\sqrt{\delta'}x_L\right)}. \quad (3.21)$$

By the same analysis that is presented for Eq.(3.6), the temperature distribution for periodic heat flux in skin tissue is

$$\begin{aligned} \theta(\xi, \eta) = & \frac{\cosh\sqrt{\frac{i(i+C')(1+A'i)}{F'i+G'-E'}}(\xi-x_L)}{\sqrt{\frac{i(i+C')(1+A'i)}{F'i+G'-E'}} \sinh\sqrt{\frac{i(i+C')(1+A'i)}{F'i+G'-E'}}x_L} e^{i\eta} - \frac{G'}{ix_L C'} + \frac{E'C'^2 - CF' + G'}{C'(C'+i)(1-A'C')x_L} e^{-C'\eta} + \\ & + \frac{E' - F'A' + G'A^2}{(1+iA')(C'A' - I)x_L} e^{-\frac{\eta}{A'}} + \sum_{m=1}^3 \sum_{n=1}^{\infty} \frac{2 \cos[\lambda_n(\xi-x_L)/x_L]}{x_L \cos(\lambda_n)} \times \\ & \times \frac{E's_{nm}^2 + F's_{nm} + G'}{(s_{nm} - i)(3A's_{nm}^2 + (2C'A' + 2E'b_n + 2)s_{nm} + C' + G'b_n)} e^{s_{nm}\eta}. \end{aligned} \quad (3.22)$$

For DPL, TW, Pennes' model

$$\begin{aligned} \theta(\xi, \eta) = & \frac{\phi\left[\left(e^{-D'\eta} - I\right) - B'D'\left(e^{-\eta/B'} - I\right)\right]}{D'(B'D' - I)} + \frac{(D'F' - I)e^{-D'\eta}}{x_L(B'D' - I)(D' - i)} + \frac{(F' - B')e^{-\eta/B'}}{x_L(B'D' - I)(1 + iB')} \times \\ & \times \frac{\cosh\left[\sqrt{\frac{D' - B' + i(B'D' + I)}{1 + iF'}}(\xi - x_L)\right] e^{i\eta}}{\sqrt{\frac{D' - B' + i(B'D' + I)}{1 + iF'}} \sinh\left(\sqrt{\frac{D' - B' + i(B'D' + I)}{1 + iF'}}x_L\right)} + \sum_{m=1}^2 \sum_{n=1}^{\infty} \frac{2 \cos[\lambda_n(\xi-x_L)/x_L]}{x_L \cos \lambda_n} \times \\ & \times \left[ \frac{(1 + F's_{nm})e^{s_{nm}\eta}}{(s_{nm} - i)(2B's_{nm} + B'D' + 1 + F'b_n)} \right] \end{aligned} \quad (3.23)$$

where

$s_{nm}$  are roots of Eq.(3.24)

$$a's_{nm}^3 + b's_{nm}^2 + c's_{nm} + d' = 0. \quad (3.24)$$

#### 4. Results and discussion

The values of applicable parameters are similar to the parameters as in the literature [35–36]. The thermophysical properties of the skin tissue are:  $k = 0.628 \text{ W.m}^{-1}.\text{K}^{-1}$ ,  $c = 4187 \text{ J.kg}^{-1}.\text{K}^{-1}$ ,  $\rho_b = 1000 \text{ kg.m}^{-3}$ ,  $c_b = 4187 \text{ J.kg}^{-1}.\text{K}^{-1}$ ,  $T_a = 37^\circ\text{C}$ ,  $\omega_b = 1.87 \times 10^{-3} \text{ s}^{-1}$ ,  $q_m = 1.19 \times 10^3 \text{ W.m}^{-3}$ ,  $T_0 = 37^\circ\text{C}$ ,  $T_w = 37^\circ\text{C}$ ,  $Q_{m0} = 1.901 \times 10^3 \text{ Wm}^{-3}$  and thickness of tissue slab is  $L = 0.05 \text{ m}$ . The intensity of pulse train incident heat flux  $q_0 = 19 \times 10^3 \text{ W/m}^2$ , and for periodic heat flux  $q_0 = 5 \times 10^3 \text{ W.m}^{-2}$  [9]. Different values of thermal relaxation times are taken in order to capture micro-structural interaction effects on the thermal behavior of skin tissue.

In this work, the temperature distributions in skin tissue based on the Pennes', TW, DPL, and TPL models are compared. TPL1 ( $\tau_q = 16s, \tau_t = 8s, \tau_v = 4s$ ), TPL2 ( $\tau_q = 16s, \tau_t = 16s, \tau_v = 4s$ ), TPL3 ( $\tau_q = 16s, \tau_t = 32s, \tau_v = 4s$ ) and flux precedence (FP  $\tau_q = 16s, \tau_t = 32s$ ), gradient precedence (GP  $\tau_q = 16s, \tau_t = 8s$ ) heat flow regimes are considered for the TPL and DPL models, respectively. TPL1, TPL2 and TPL3 are notations used for heat flow regimes in the TPL model. A validation procedure as in [24] is performed and a comparison is made between the results obtained TPL and DPL models.

Figure 1a shows that variation of the tissue temperature for three different types of heat regimes in the case of the TPL model for  $k^* = 0.01 W.m^{-1}.K^{-1}s^{-1}$ . The tissue temperature is higher for TPL3 type heat flow regime than other regimes. Figures 1b and 1c indicate the similarity of the tissue temperature for the case of pulse train and periodic heat flux, respectively. These figures clearly show that when proper restrictions are applied to the solution of the TPL model, the results show good agreement with the solution of Pennes', TW, and DPL models. The tissue temperature is influenced by the value of the material constant  $k^*$  as noticed in Fig.1c.

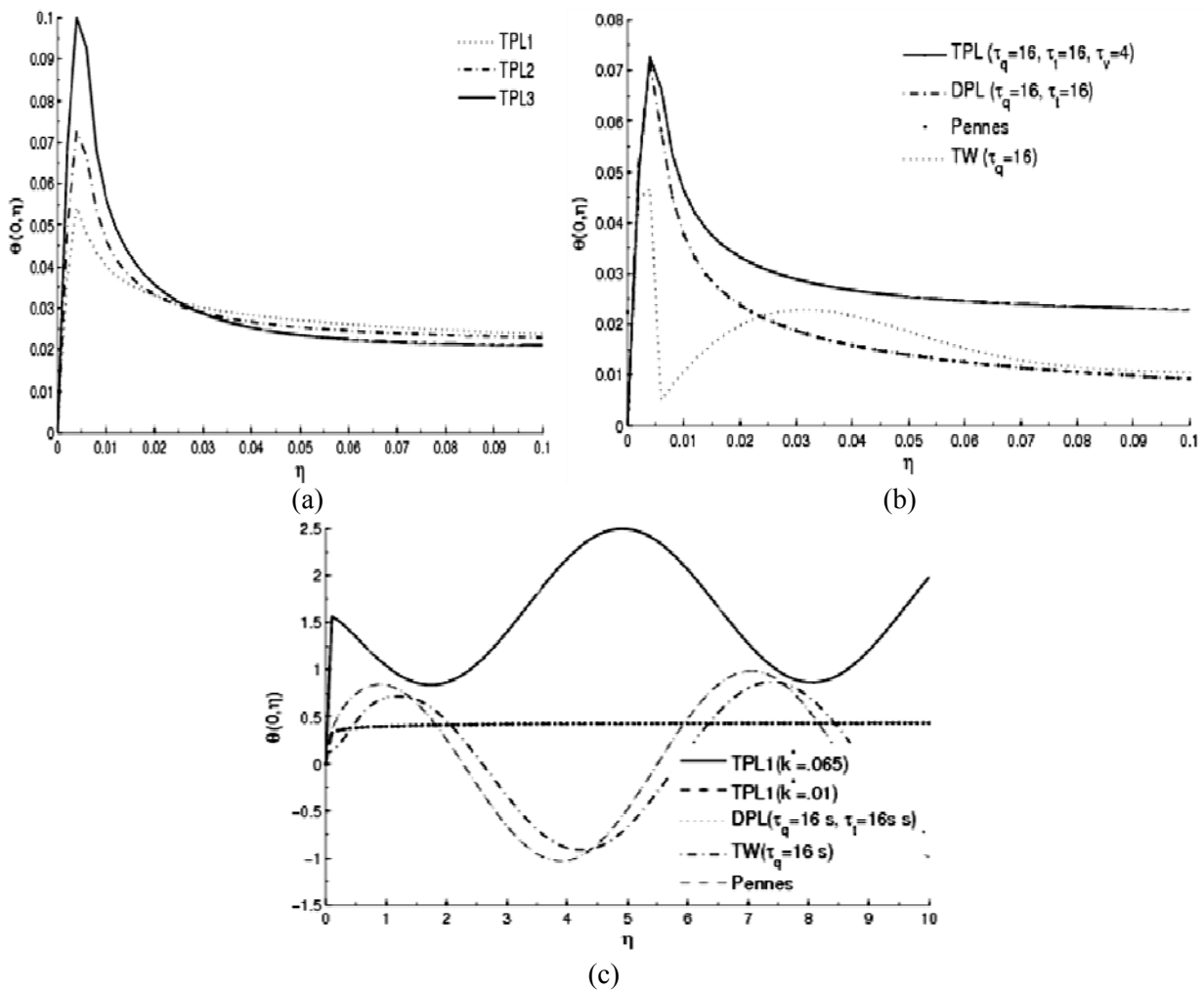
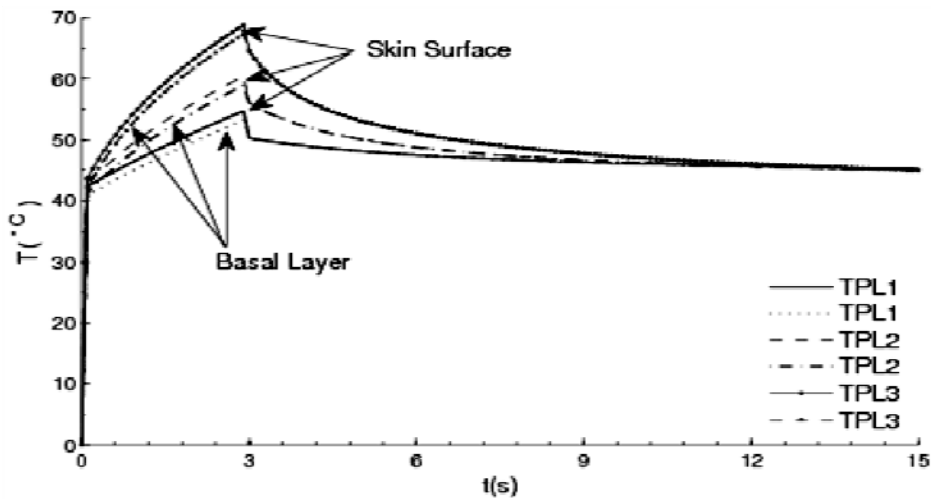
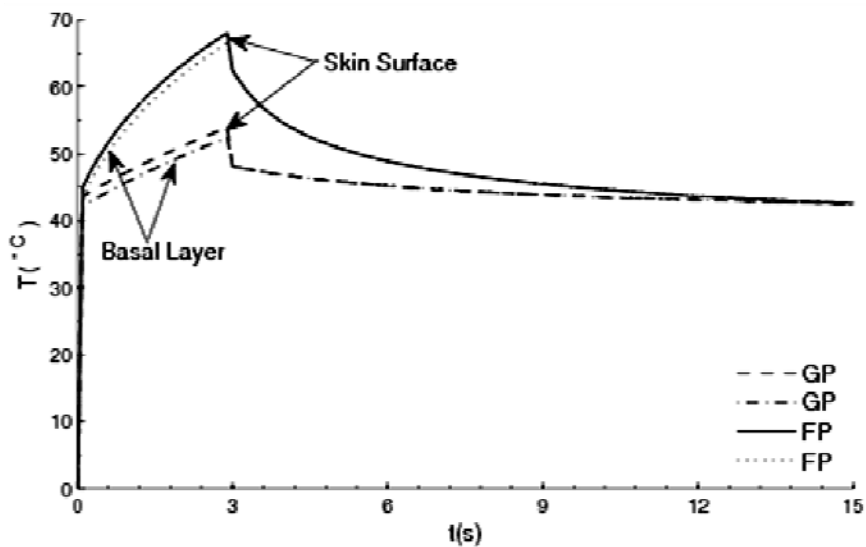


Fig. 1a. Tissue temperature responses subjected to pulse train heat flux predicted by the TPL1, TPL2 and TPL3 type heat flow regimes, Fig.1b. Tissue temperature responses subjected to a pulse train heat flux predicted by TPL, DPL, TW, and Pennes' models for limiting cases, Fig.1c. Tissue temperature responses subjected to a periodic heat flux predicted by TPL, DPL, TW, and Pennes' models for limiting cases.

Figures 2a and 2b show the tissue temperature predicted at the skin surface and basal layer ( $x = 80 \times 10^{-6} \text{ m}$ ) Ahmadikia *et al.* [17] for TPL and DPL models when the skin tissue is exposed to a pulse train heat flux with exposed time  $\tau_i = 3 \text{ s}$  with ( $k^* = 0.01 \text{ W} \cdot \text{m}^{-1} \cdot \text{K}^{-1} \cdot \text{s}$ ). These figures clearly show that the TPL model predicts a higher temperature in TPL3 type of heat flow regime than that of TPL1 and TPL2 regimes and temperature becomes constant at  $t = 12 \text{ s}$  and  $t = 13 \text{ s}$  for TPL and DPL models, respectively. It is evident that physical understanding of the tissue thermal behavior strongly depends on the values of the thermal displacement gradient, temperature gradient, and heat flux relaxation times ( $\tau_v$ ,  $\tau_t$ , and  $\tau_q$ ).



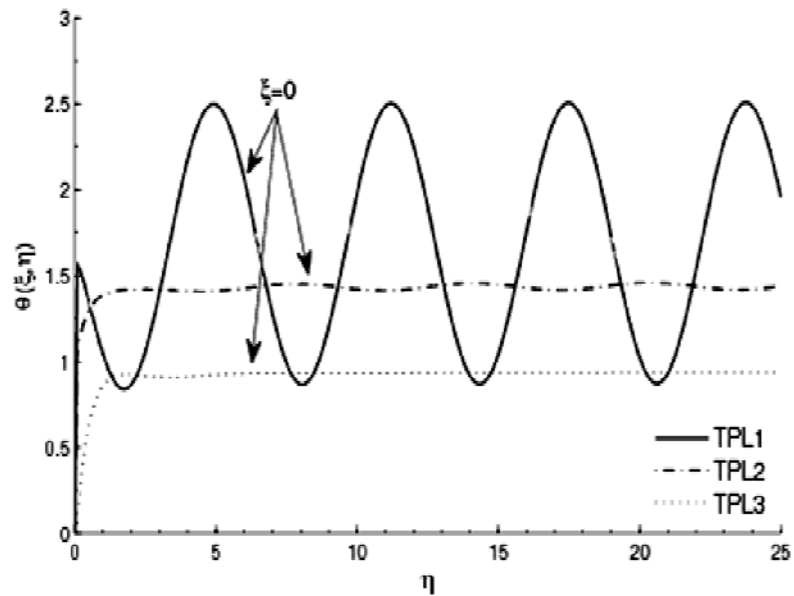
(a)



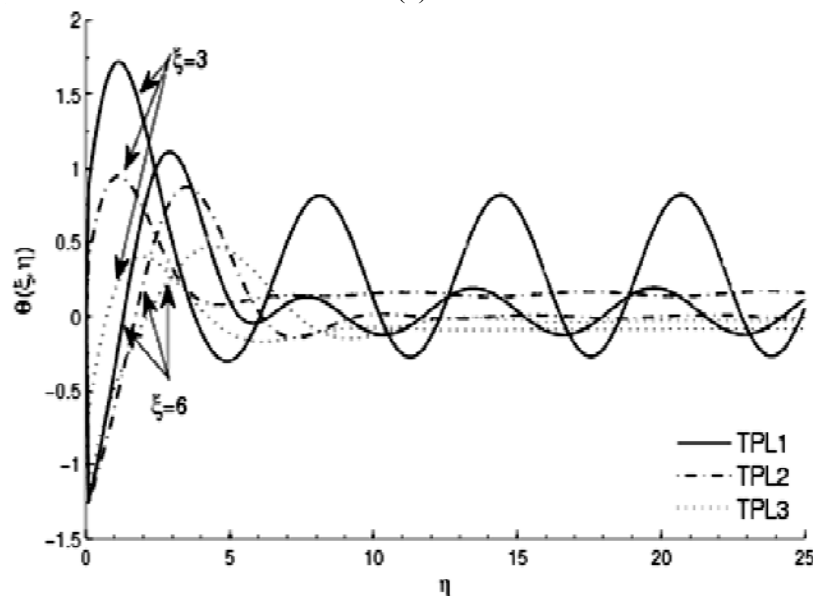
(b)

Fig. 2a. Tissue temperature predicted by TPL model for TPL1, TPL2, and TPL3 heat flow regimes at the skin surface and basal layer exposed to a pulse train heat flux, Fig.2b. Tissue temperature predicted by DPL model for GP and FP heat flow regimes at the skin surface and basal layer exposed to a pulse train heat flux.

Figures 3a and 3b show the temperature responses of the skin tissue subjected to a periodic surface heat flux predicted by the TPL model at three different depths beneath the skin surface when  $\omega = 0.05 \text{ s}^{-1}$  and  $k^* = 0.065 \text{ W.m}^{-1}.\text{K}^{-1}.\text{s}^{-1}$ . It is noticed from these figures that the oscillatory amplitude of the tissue becomes low for a large depth from the heating skin in all three regimes, but higher than the temperature predicted by the DPL model in both regimes. It means that the influence of relaxation times on the tissue temperature amplitude is more important at the locations which are near the skin surface.



(a)



(b)

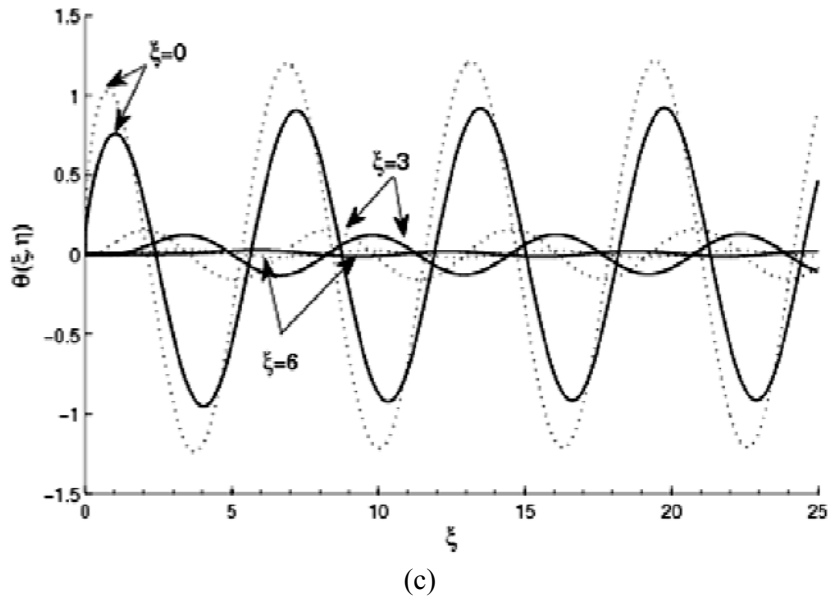
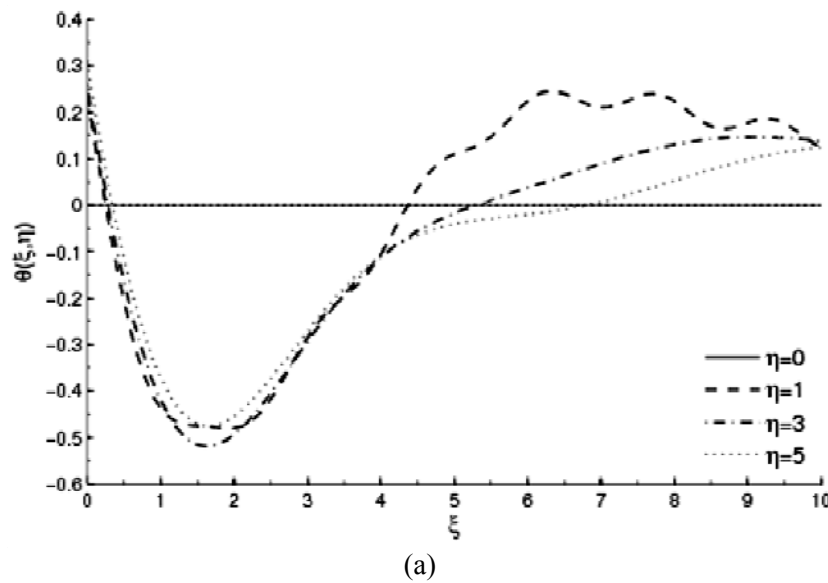


Fig. 3a, Fig.3b Tissue temperature responses in different distances beneath the skin surface exposed to a periodic heat flux predicted by the TPL model. Figure 3c. Tissue temperature responses in different distances beneath the skin surface exposed to a periodic heat flux predicted by the DPL model.

Figures 4a, 4b, and 4c depict the dimensionless tissue temperature along the dimensionless distance changed with different dimensionless times predicted by the TPL model when  $\omega = 0.05 \text{ s}^{-1}$  and  $k^* = 0.01 \text{ W.m}^{-1}.\text{K}^{-1}.\text{s}^{-1}$ . The tissue temperature decreases from  $\xi = 0$  to  $\xi = 1.5$  in all heat regimes TPL1, TPL2 and TPL3. In TPL3 type heat regime the dimensionless tissue temperature becomes constant for  $\xi > 6$  and seems to be independent of the oscillatory heat flux on the heating skin, but for  $\xi < 6$  the effect of periodic heat flux on the tissue temperature is profound. Figure 4d predicts that the tissue temperature is affected by the value of  $\tau_t$  near  $\xi = 0$  in the case of the DPL model and other results are similar to the results predicted by the TPL model.



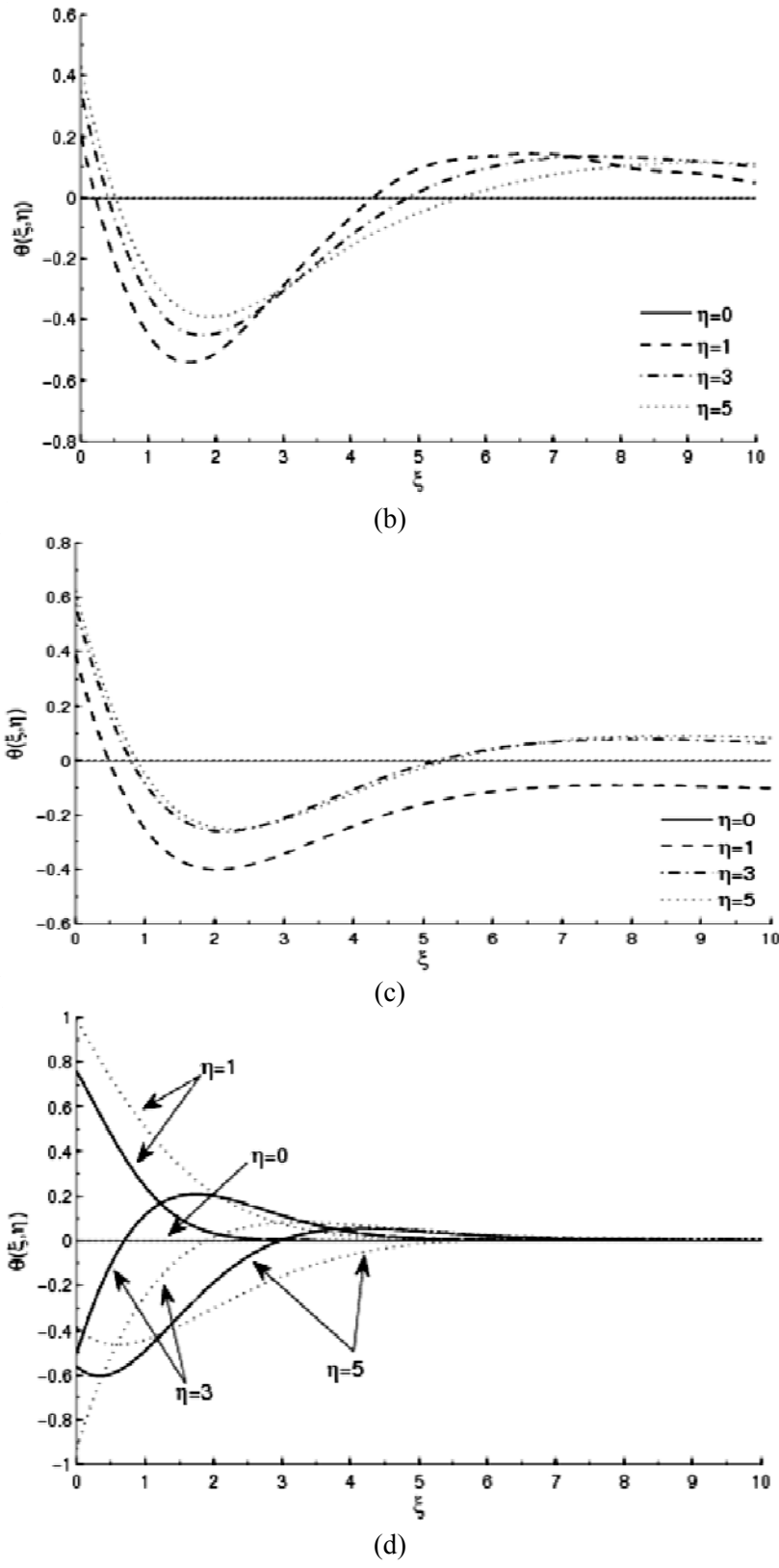


Fig.4. Tissue temperature profile along the tissue depth at different phase angles: Fig.4a for TPL1 heat flow regime, 4b. for TPL2 heat flow regime, 4c. for TPL3 heat flow regime and Fig.4d. for the DPL model in GP( solid line) and FP (dotted line) heat flow regimes.

Figures 5a and 5b indicate the temperature profile along the tissue depth predicted by the TPL and DPL models at different frequencies of periodic heat flux when  $\eta = 2\pi$ . It is clear from the figure that the oscillatory effects decrease along the tissue depth. The temperature predicted by the TPL model is higher than the DPL model in all three types of heat glow regimes.

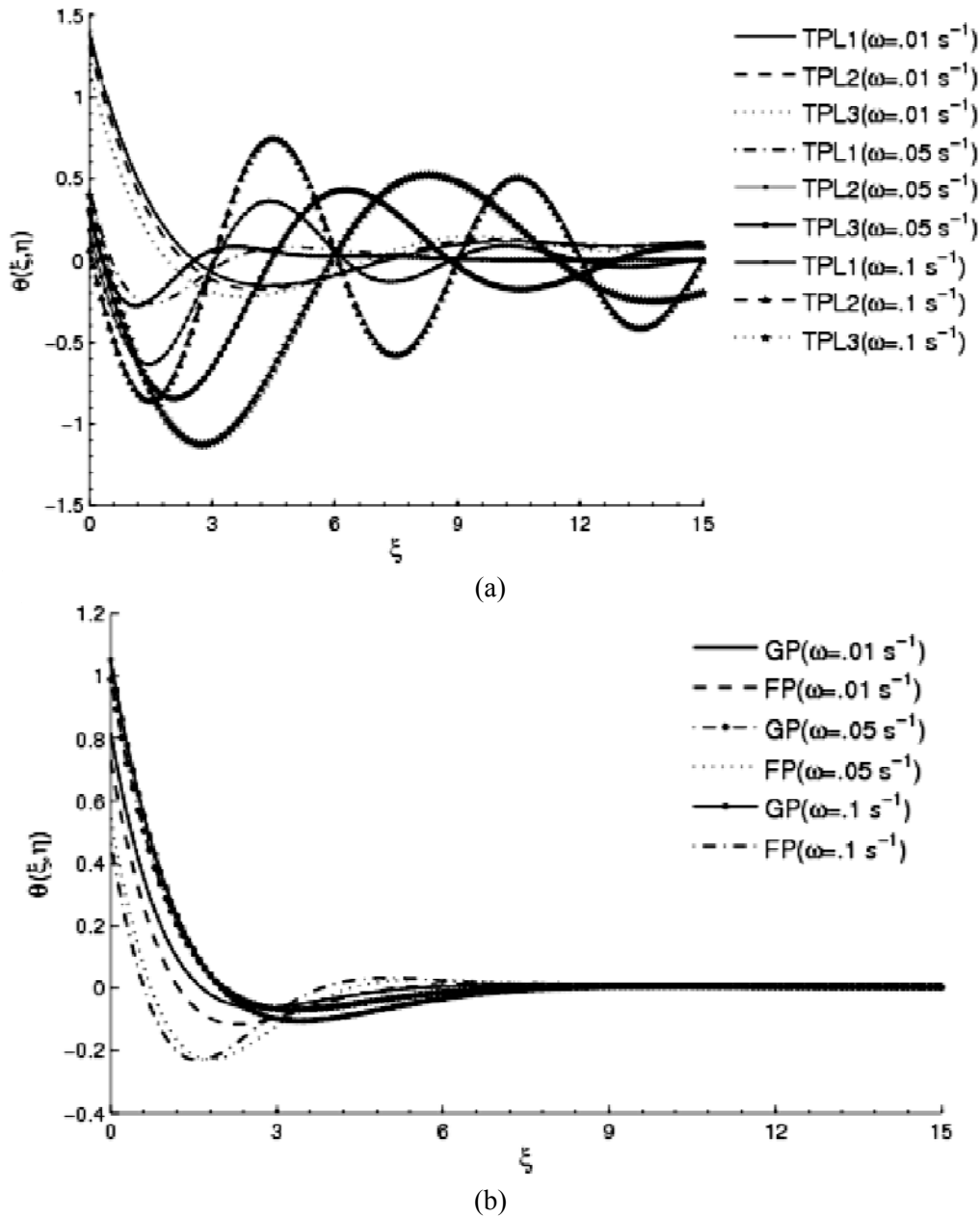
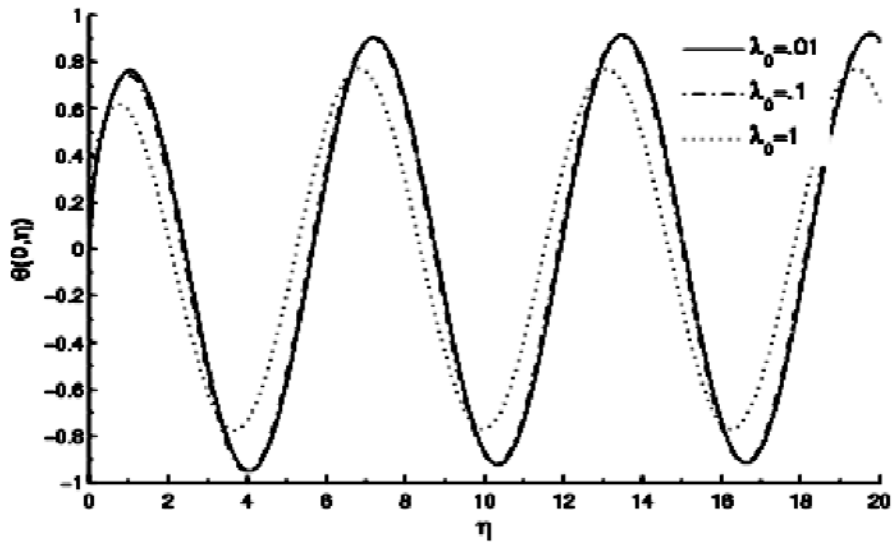


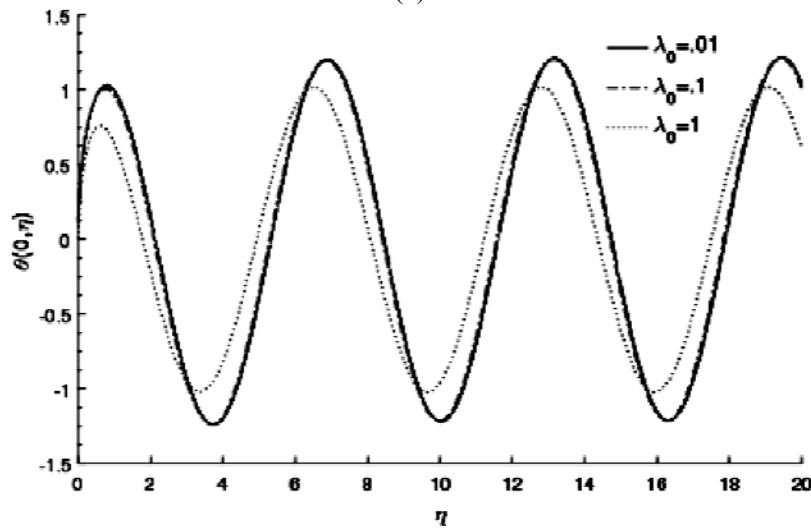
Fig.5. Temperature profile along the tissue depth at different frequencies of periodic heat flux in the skin surface when  $\eta = 2\pi$  predicted by: Fig.5a. for TPL model and Fig.5b. for DPL model.

Figures 6a, 6b and Figs 7a, 7b and 7c show the dimensionless temperature profile on the skin surface predicted by the DPL and TPL models respectively, with different dimensionless blood perfusion values when  $\omega = 0.05 \text{ s}^{-1}$ . The lines with  $\lambda_0 = 0.01$  and  $0.1$  coincide with each other for the DPL model but are different in the case of the TPL model. There is no similarity between the temperature responses at the skin

surface predicted by the TPL and DPL models with these blood perfusion values but independently it influences the temperature responses.

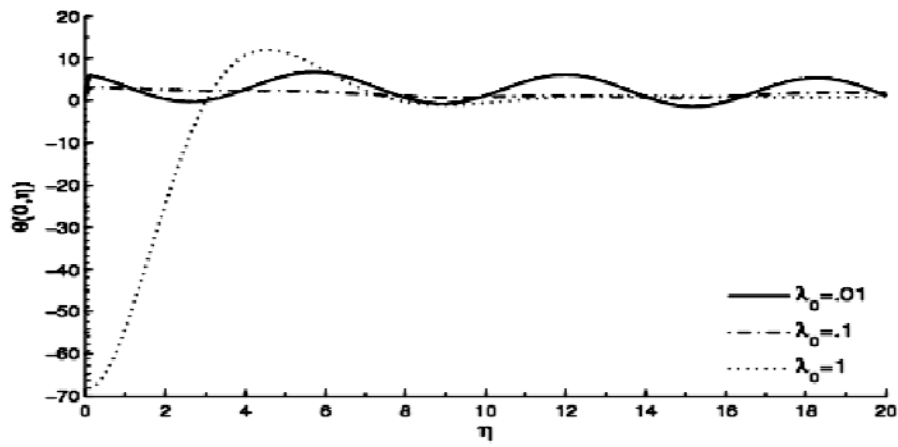


(a)

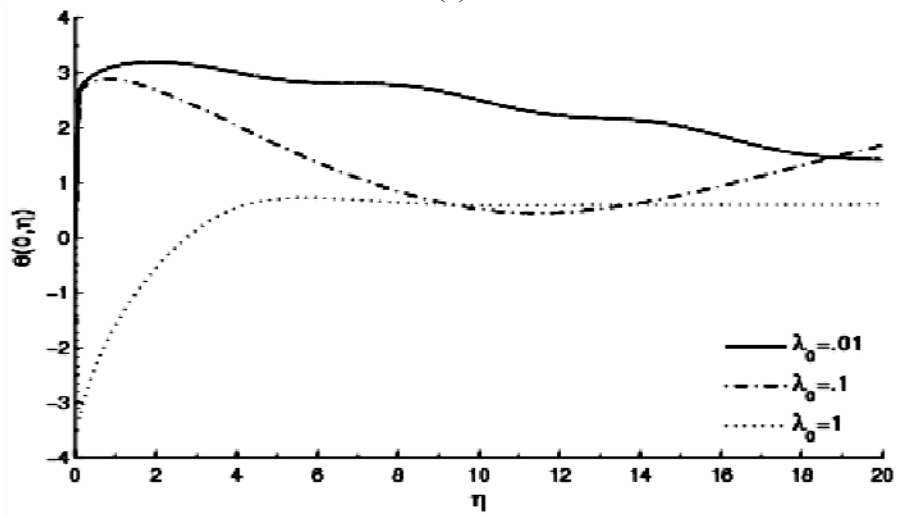


(b)

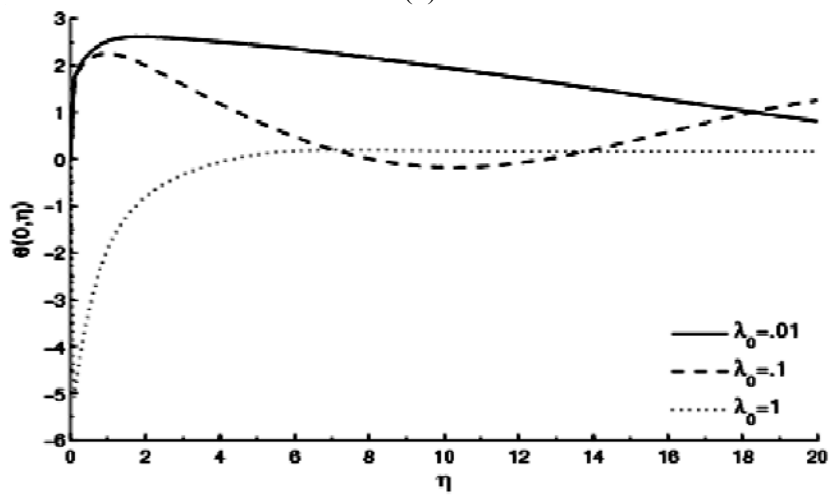
Fig.6a. Predicts tissue temperature responses on the skin surface for different values of  $\lambda_0$  in GP heat flow regime by DPL model. Fig. 6b predicts tissue temperature responses on the skin surface for different values of  $\lambda_0$  in FP heat flow regime by DPL model.



(a)



(b)



(c)

Fig.7. Tissue temperature responses on skin surface for different value of  $\lambda_0$  predicted by: Fig.7a. for TPL1, Fig.7b for TPL2 and Fig.7c for TPL3 heat flow regimes.

## 5. Conclusions

Heat transfer process and temperature distribution in skin tissue is important in thermal therapeutic applications. This work employed the three-phase-lag (TPL), dual-phase-lag (DPL), thermal wave (TW), and Pennes' models of the bioheat transfer equation in a finite length skin tissue. An exact analytical solution is obtained with given initial and boundary conditions. A good agreement exists between the results, obtained from the TPL and DPL models for limiting cases. Tissue thermal behavior is significantly affected by phase-lag parameters and material constant. TPL3 type heat flow regime predicts a higher temperature than other regimes for both pulse train and periodic heat flux. The depth of skin is influenced by the different oscillation heat flux and oscillatory effect decreases along the tissue depth. The temperature profile shows different behavior for the dimensionless blood perfusion rate in the TPL and DPL models at the skin surface. This work can be extended to study the neuro-physiological behavior of the skin tissue under different thermomechanical loading.

## Acknowledgments

The third author is thankful to the Council of Scientific and Industrial Research (CSIR), India, for providing fellowship under the JRF(21/06/2015/(i)EU-V) scheme.

## Nomenclature

- $c$  – tissue specific heat ( $J.kg^{-1}.K^{-1}$ )
- $c_b$  – blood specific heat ( $J.kg^{-1}.K^{-1}$ )
- $k$  – thermal conductivity of tissue ( $W.m^{-1}.K^{-1}$ )
- $k^*$  – material constant ( $W.m^{-1}.K^{-1}.s^{-1}$ )
- $L$  – tissue slab length ( $m$ )
- $l$  – Bromwich contour integration line
- $p_m$  – dimensionless metabolic heat generation for TPL model Eq.(3.2)
- $Q$  – heat flux density ( $W.m^{-2}$ )
- $Q_{m0}$  – basal metabolic heat generation rate ( $W.m^{-3}$ )
- $q_0$  – incident heat flux amplitude ( $W.m^{-2}$ )
- $q_m$  – heat source due to metabolic heat generation in the tissue ( $W.m^{-3}$ )
- $s$  – Laplace domain parameter
- $T$  – tissue temperature ( $^{\circ}C$ )
- $T_0$  – initial tissue temperature ( $^{\circ}C$ )
- $T_a$  – arterial blood temperature ( $^{\circ}C$ )
- $T_w$  – vessel wall temperature ( $^{\circ}C$ )
- $t$  – time ( $s$ )
- $U$  – unit step function
- $x$  – coordinate variable ( $m$ )
- $x_L$  – dimensionless tissue slab length
- $\alpha$  – tissue thermal diffusivity ( $m^2.s^{-1}$ )

- $\Gamma_i$  – dimensionless incident heat flux exposure time  
 $\theta$  – dimensionless tissue temperature  
 $\lambda_0$  – dimensionless blood perfusion rate  
 $\xi$  – dimensionless coordinate  
 $\rho$  – tissue density ( $kg\ m^{-3}$ )  
 $\rho_b$  – blood mass density ( $kg\ m^{-3}$ )  
 $\tau_i$  – duration of pulse train heat flux (s)  
 $\tau_q$  – heat flux relaxation time (s)  
 $\tau_t$  – temperature gradient relaxation time (s)  
 $\tau_v$  – thermal displacement relaxation time (s)  
 $\tau_l$  – dimensionless heat flux relaxation time  
 $\tau_2$  – dimensionless temperature gradient relaxation time  
 $\tau_3$  – dimensionless thermal displacement relaxation time  
 $\phi$  – dimensionless metabolic heat generation Eq.(3.18)  
 $\psi$  – dimensionless metabolic heat generation Eq.(3.2)  
 $\omega$  – incident heat flux frequency ( $s^{-1}$ )  
 $\omega_b$  – blood perfusion rate ( $s^{-1}$ )

## References

- [1] Pennes H.H. (1948): *Analysis of tissue and arterial blood temperature in the resting forearm.* – J. Appl. Physiol., vol.1, pp.93-122.
- [2] Cattaneo C. (1958): *A form of heat conduction equation which eliminates the paradox of instantaneous propagation.* – Comp. Rend., vol.247, pp.431-433.
- [3] Vernotte P. (1958): *Les paradoxes de la theorie continue de l'equation de la chaleur.* – Comp. Rend., vol.246, pp.3154-3155.
- [4] Tzou D.Y. (1995): *Macro-to Microscale Heat transfer: The Lagging Behavior.* – Washington: Taylor and Francis.
- [5] Tzou D.Y. (1995): *A unified field approach for heat conduction from macro-to-microscales.* – ASME J. Heat Transf., vol.117, pp.8-16.
- [6] Roy Choudhuri S.K. (2007): *On a thermoelastic three-phase-lag model, journal of thermal stresses.* – J. Therm. Stress, vol.30, pp.231-238.
- [7] Sur Abhik and Kanoria M. (2015): *Analysis of thermoelastic response in a functionally graded infinit space subjected to a Mode-I crack.* – Int. J. Adv. Appl. Math. Mech, vol.3, pp.33-44.
- [8] Kumar R. and Gupta V. (2016): *Plane wave propagation and domain of influence in fractional order thermoelastic materials with three-phase-lag heat transfer.* – Mech. Adv. Mater. Struct., vol.23, pp.896-908.
- [9] Shih T.C., Yuan P., Lin W.L. and Kou H.S. (2007): *Analytical analysis of the Pennes bioheat transfer equation with sinusoidal heat flux condition on skin surface.* – Med. Eng. Phys., vol.29, pp.946-953.
- [10] Zhang Y., Chen J.K. and Zhou J. (2009): *Dual-phase lag effects on thermal damage to biological tissues caused by laser irradiation.* – Comput. Biol. Med., vol.39, pp.286-293.
- [11] Zhou J., Zhang Y. and Chen J.K. (2009): *An axisymmetric dual-phase-lag bioheat model for laser heating of living tissues.* – Int. J. Therm. Sci., vol.48, pp.1477-1485.
- [12] Zhang Y. (2009): *Generalized dual-phase lag bioheat equations based on nonequilibrium heat transfer in living biological tissues.* – Int. J. Heat Mass Transf., vol.52, pp.4829-4834.

- [13] Liu K.C. and Chen H.T. (2009): *Analysis for dual phase lag bioheat transfer during magnetic hyperthermia treatment*. – Int. J. Heat Mass Transf, vol.52, pp.1185-1192.
- [14] Majchrzak J.E. (2010): *Numerical solution of dual phase lag model of bioheat transfer using the general boundary element method*. – Comput. Modeling Eng. Sci., vol.69, pp.43-60.
- [15] Poor H.Z., Moosavi H. and Moradi A. (2014): *Investigation on the dual-phase-lag effects in biological tissues during laser irradiation*. – Int. J. Mech. Syst. Eng., vol.4, pp.33-46.
- [16] Majchrzak E. and Turchan L. (2015): *The general boundary element method for 3D dual-phase lag model of bioheat transfer*. – Eng. Anal. with Boundary Elements., vol.50, pp.76-82.
- [17] Ahmadikia H., Fazlali R. and Moradi A. (2012): *Analytical solution of the parabolic and hyperbolic heat transfer equations with constant and transient heat flux conditions on skin tissue*. – Int. Commun Heat Mass Transf., vol.39, pp.121-130.
- [18] Ahmadikia H., Moradi A., Fazlali R. and Parsa A.B. (2012): *Analytical solution of non-Fourier and Fourier bioheat transfer analysis during laser irradiation of skin tissue*. – J. Mech. Sci. Technol., vol.26, pp.1937-1947.
- [19] Afrin N., Zhou J., Zhang Y, Tzou D.Y. and Chen J.K. (2012): *Numerical simulation of thermal damage to living tissues induced by laser irradiation based on a generalized dual phase lag model*. – Numer. Heat Transf., vol.61, pp.483-501.
- [20] Kengne E., Lakhssassi A. and Vaillancourt R. (2012): *Temperature distribution in living biological tissue simultaneously subjected to oscillatory surface and spatial heating: analytical and numerical analysis*. – Int. Mathematical Forum., vol.7, pp.2373-2392.
- [21] Fazlali R. and Ahmadikia H. (2013): *Analytical solution of thermal wave models on skin tissue under arbitrary periodic boundary conditions*. – Int. J. Thermophys., vol.34, pp.139-159.
- [22] Shahnazari M., Aghanajafi C., Azimifar M. and Jamali H. (2013): *Investigation of bioheat transfer equation of Pennes via a new method based on wrm and homotopy perturbation*. – IJRRAS, vol.17, pp.306-314.
- [23] Gupta P.K., Singh J., Rai K.N. and Rai S.K. (2013): *Solution of the heat transfer problem in tissues during hyperthermia by finite difference-decomposition method*. – Appl. Math. Comput., vol.219, pp.6882-6892.
- [24] Askarizadeh H. and Ahmadikia H. (2014): *Analytical analysis of the dual-phase-lag model of bioheat transfer equation during transient heating of skin tissue*. – Heat Mass Transf., vol.50, pp.1673-1684.
- [25] Kengne E., Mellal I., Hamouda M.B. and Lakhssassi A. (2014): *A mathematical model to solve bio-heat transfer problems through a bio-heat transfer equation with quadratic temperature-dependent blood perfusion under a constant spatial heating on skin surface*. – J. Biom. Sci. Eng., vol.7, pp.721-730.
- [26] Kumar P., Kumar D. and Rai K.N. (2015): *A numerical study on dual-phase-lag model of bio-heat transfer during hyperthermia treatment*. – J. Therm. Biol., vol.49-50, pp.98-105.
- [27] Majchrzak E., Turchan L. and Dziatkiewicz J. (2015): *Modeling of skin tissue heating using the generalized dual phase-lag equation*. – Arch. Mech., vol.67, pp.417-437.
- [28] Jasinski M., Majchrzak E. and Turchan L. (2016): *Numerical analysis of the interactions between laser and soft tissue using generalized dual-phase-lag equation*. – Appl. Math. Model., vol.40, pp.750-762.
- [29] Kumar D. and Rai K.N. (2016): *A study on thermal damage during hyperthermia treatment based on DPL model for multilayer tissues using finite element Legendre wavelet Galerkin approach*. – J. Therm. Biol., vol.62, pp.170-180.
- [30] Agrawal M. and Pardasani K.R. (2016): *Finite element model to study temperature distribution in skin and deep tissues of human limbs*. – J. Therm. Biol., vol.62, pp.98-105.
- [31] Green A.E. and Naghdi P.M. (1992): *On undamped heat waves in an elastic solid*. – J. Therm. Stress., vol.15, pp.253-264.
- [32] Green A.E. and Naghdi P.M. (1993): *Thermoelasticity without energy dissipation*. – J. Elast., vol.31, pp.189-208.

- [33] Mitchell J.W., Galvez T.L., Hangle J., Myers G.E. and Siebecker K.L. (1970): *Thermal response of human legs during cooling*. – J. Appl. Physiol., vol.29, pp.859-865.
- [34] Arpaci V.C. (1996): *Conduction heat transfer*. – New York: Addison Wesley.
- [35] Yamada Y., Tien T. and Ohta M. (1995): *Theoretical analysis of temperature variation of biological tissue irradiated by light*. – ASME/JSME Thermal Eng. Con, vol.4, pp.575-581.
- [36] Torvi D.A. and Dale J.D. (1994): *A finite element model of skin subjected to a flash fire*. – ASME J. Biomech. Eng., vol.116, pp.250-255.

Received: January 11, 2018

Revised: April 4, 2019